

Characterizing Continental US Hurricane Risk: Which Intensity Metric is Best?

Philip J Klotzbach¹, Daniel Chavas², Michael Bell¹, Steven G. Bowen³, Ethan J Gibney⁴, and Carl Schreck⁵

¹Colorado State University

²Purdue University

³Aon

⁴Cooperative Programs for the Advancement of Earth System Science

⁵North Carolina State University

November 30, 2022

Abstract

The damage potential of a hurricane is widely considered to depend more strongly on an integrated measure of the hurricane wind field, such as Integrated Kinetic Energy (IKE), than a point-based wind measure, such as maximum sustained wind speed (V_{\max}). Recent work has demonstrated that minimum sea level pressure (MSLP) is also an integrated measure of the wind field. This study investigates how well historical continental US hurricane damage is predicted by MSLP compared to both V_{\max} and IKE for continental United States hurricane landfalls for the period 1988–2020. We first show for the entire North Atlantic basin that MSLP is much better correlated with IKE ($r_{rank} = 0.50$) than V_{\max} ($r_{rank} = 0.26$). We then show that continental US hurricane normalized damage is better predicted by MSLP ($r_{rank} = 0.81$) than either V_{\max} ($r_{rank} = 0.65$) or IKE ($r_{rank} = 0.68$). For Georgia to Maine hurricane landfalls specifically, MSLP and IKE show similar levels of skill at predicting damage, whereas V_{\max} provides effectively no predictive power. Conclusions for IKE extend to power dissipation as well, as the two quantities are highly correlated because wind radii closely follow a Rankine vortex. The physical relationship of MSLP to IKE and power dissipation is discussed. In addition to better representing damage, MSLP is also much easier to measure via aircraft or surface observations than either V_{\max} or IKE, and it is already routinely estimated operationally. We conclude that MSLP is an ideal metric for characterizing hurricane damage risk.

1 **Characterizing Continental US Hurricane Risk: Which Intensity Metric is**
2 **Best?**

3
4
5 **Philip J. Klotzbach¹, Daniel R. Chavas², Michael M. Bell¹, Steven G. Bowen³, Ethan J.**
6 **Gibney⁴, and Carl J. Schreck III⁵**

7 ¹Department of Atmospheric Science, Colorado State University, Fort Collins, CO, USA.

8 ²Department of Earth, Atmospheric and Planetary Sciences, Purdue University, West Lafayette,
9 IN, USA.

10 ³Aon, Chicago, IL, USA.

11 ⁴Cooperative Programs for the Advancement of Earth System Science, UCAR, San Diego, CA,
12 USA.

13 ⁵Cooperative Institute for Satellite Earth System Studies (CISESS), North Carolina State
14 University, Asheville, NC, USA.

15
16 Corresponding author: Philip Klotzbach (philk@atmos.colostate.edu)

17 **Key Points:**

- 18 • Minimum sea level pressure better predicts continental US hurricane damage than
19 maximum winds or integrated kinetic energy.
- 20 • Maximum winds have historically been a poor predictor of damage caused by hurricanes
21 making landfall from Georgia to Maine.
- 22 • Minimum sea level pressure is intrinsically an integrated wind field metric and is easy to
23 measure, ideal for categorizing hurricane risk.
24

25 Abstract

26 The damage potential of a hurricane is widely considered to depend more strongly on an
27 integrated measure of the hurricane wind field, such as Integrated Kinetic Energy (IKE), than a
28 point-based wind measure, such as maximum sustained wind speed (V_{\max}). Recent work has
29 demonstrated that minimum sea level pressure (MSLP) is also an integrated measure of the wind
30 field. This study investigates how well historical continental US hurricane damage is predicted
31 by MSLP compared to both V_{\max} and IKE for continental United States hurricane landfalls for
32 the period 1988–2020. We first show for the entire North Atlantic basin that MSLP is much
33 better correlated with IKE ($r_{rank} = 0.50$) than V_{\max} ($r_{rank} = 0.26$). We then show that continental
34 US hurricane normalized damage is better predicted by MSLP ($r_{rank} = 0.81$) than either V_{\max}
35 ($r_{rank} = 0.65$) or IKE ($r_{rank} = 0.68$). For Georgia to Maine hurricane landfalls specifically, MSLP
36 and IKE show similar levels of skill at predicting damage, whereas V_{\max} provides effectively no
37 predictive power. Conclusions for IKE extend to power dissipation as well, as the two quantities
38 are highly correlated because wind radii closely follow a Modified Rankine vortex. The physical
39 relationship of MSLP to IKE and power dissipation is discussed. In addition to better
40 representing damage, MSLP is also much easier to measure via aircraft or surface observations
41 than either V_{\max} or IKE, and it is already routinely estimated operationally. We conclude that
42 MSLP is an ideal metric for characterizing hurricane damage risk.

43

44 Plain Language Summary

45

46 For decades, maximum sustained winds have been used to categorize potential hurricane
47 impacts. Recent work argues that an integrated hurricane wind field measure better represents
48 risk. Here we use historical continental U.S. hurricane and economic damage data to show that
49 minimum sea level pressure better correlates with damage than integrated kinetic energy, a
50 measure of hurricane vortex size and strength, or maximum sustained wind. Maximum sustained
51 wind has been a poor damage predictor for Georgia to Maine landfalling hurricanes. Since
52 minimum central pressure is an integrated wind field measure that only requires storm center
53 measurements, and is already routinely estimated, we propose that minimum sea level pressure
54 replace maximum sustained wind as the primary hurricane categorization method.

55

56 **1 Introduction**

57 Hurricanes are one of the most damaging natural catastrophes, causing hundreds to thousands of
58 fatalities and billions of US dollars (USD) in damage globally each year (Mendelsohn et al.,
59 2012; Klotzbach et al., 2018; Grinsted et al., 2019). Damage from hurricanes has grown in recent
60 years, with a primary driver being an increase in population and wealth along the coast. Given
61 the large impacts that hurricanes cause, ideally their intensity should be categorized using
62 metrics that best represent their potential impacts when communicating risk to the public.

63 For more than 40 years, North Atlantic (hereafter Atlantic) and eastern North Pacific hurricanes
64 have been categorized using the Saffir–Simpson Hurricane Scale (Simpson, 1974), although the
65 utility of this scale has been called into question during the past ~15 years. In 2010, the National
66 Hurricane Center removed storm surge and minimum sea level pressure (MSLP) from the scale,
67 resulting in the modified Saffir–Simpson Hurricane Wind Scale (SSHWS; Schott et al., 2012),
68 which categorizes hurricanes purely based on maximum sustained wind (V_{\max}).

69 Powell and Reinhold (2007) advocated for an integrated kinetic energy (IKE) metric to
70 categorize wind potential destruction from hurricanes. Many follow-up studies have also used
71 IKE to categorize both individual hurricanes as well as entire hurricane seasons (e.g., Maclay et
72 al., 2008; Misra et al., 2013; Kozar et al., 2014; Buchanan et al., 2018). Unlike V_{\max} , which
73 simply represents a point-based estimate of the maximum sustained winds in a hurricane, IKE
74 assesses the strength of the overall hurricane circulation. For a given V_{\max} , larger storms
75 typically have increased storm surge (Irish et al., 2008) and larger wind and rainfall footprints
76 (Lonfat et al., 2007).

77 Chavas et al. (2017) demonstrated that MSLP also intrinsically represents an integrated measure
78 of the wind field that captures the combined effect of V_{\max} and storm size. Specifically, the
79 relationship between the hurricane’s central pressure deficit (e.g., the difference in pressure
80 between the center of the hurricane and the surrounding environment) and V_{\max} can be
81 understood through gradient wind balance. The central pressure deficit increases predominantly
82 with increasing V_{\max} (the canonical “wind–pressure relationship”; Knaff and Zehr (2007))
83 but also with increasing storm size as well as background rotation rate. Hence, MSLP ought to be
84 more similar to an IKE-type metric than V_{\max} .

85 Klotzbach et al. (2020) showed that MSLP had a statistically significant improvement in
86 correlation with normalized continental US (CONUS) landfalling hurricane damage (Weinkle et
87 al., 2018) relative to V_{\max} from 1900–2018 as well as direct fatalities from 1988–2018. In
88 addition to CONUS landfalling hurricane damage, they also found a stronger relationship
89 between MSLP and a hurricane’s average 34-kt wind radii at landfall, providing additional
90 verification of Chavas et al. (2017)’s study and further evidence that MSLP may be more similar
91 to IKE than V_{\max} . To date, though, a full comparison of the utility of MSLP, V_{\max} , and IKE at
92 predicting historical damage has yet to be undertaken.

93 The purpose of this manuscript is to examine how well MSLP predicts historical damage as
94 compared to V_{\max} and IKE for CONUS landfalling hurricanes. We first compare the three
95 metrics for all Atlantic hurricanes, then likely well-monitored hurricanes in the southwestern
96 portion of the basin and then lastly for CONUS landfalling hurricanes. We then compare how
97 well each quantity predicts historical damage both overall and for Texas to Florida vs. Georgia to

98 Maine events. We also discuss the physical relationship between V_{\max} , MSLP, IKE and power
 99 dissipation (PD; Bister & Emanuel, 1998; Emanuel, 1999).

100 **2 Data and Methodology**

101 The primary dataset for the analysis that follows is the Extended Best Track (Demuth et al.,
 102 2006) that consists of intensity, location and various wind radii measurements. The location and
 103 intensity information in the extended best track are the same as in HURDAT2 (Landsea &
 104 Franklin, 2013) - NOAA's official Atlantic hurricane database. The Extended Best Track also
 105 provides 34-kt, 50-kt, and 64-kt wind radii as well as the radius of maximum winds at 6-hourly
 106 temporal resolution since 1988. Wind radii from 1988–2003 in the Extended Best Track are from
 107 operational estimates, while the National Hurricane Center has best-tracked wind radii since
 108 2004. Here we investigate the relationship between MSLP, V_{\max} and IKE in both the Extended
 109 Best Track for all Atlantic hurricanes, hurricanes in the southwest Atlantic that were likely well
 110 measured, as well as CONUS landfalling hurricanes specifically, from 1988–2020.

111 The southwest Atlantic hurricane dataset is classified using the following criteria from Chavas
 112 and Knaff (2022):

- 113 1) Take only hurricanes from 2004 onwards, as wind radii have been best tracked by the
 114 National Hurricane Center since that time
- 115 2) Select only hurricane positions where the center was located at or south of 30°N, to reduce
 116 any signal from extratropical transition
- 117 3) Take only hurricanes where the center was located at or west of 50°W, since these storms are
 118 more likely to have been observed by aircraft reconnaissance
- 119 4) Remove any hurricane locations whose distance to land is less than its mean R_{34kt} value, to
 120 reduce potential land interaction impacts on wind radii

121 Continental US landfalling hurricane MSLP and V_{\max} are taken from the Atlantic Oceanographic
 122 and Meteorological Laboratory website:

123 https://www.aoml.noaa.gov/hrd/hurdat/UShurrs_detailed.html that is based on HURDAT2. As
 124 was done in Klotzbach et al. (2020), we do count Sandy (2012) as a hurricane landfall, since it
 125 brought severe damage to the mid-Atlantic states and was a hurricane until just a few hours
 126 before landfall when it became extratropical.

127 Normalized damage estimates, that is, the amount of damage a hurricane would likely cause if it
 128 were to make landfall today given inflation and changes in exposure, are taken from Weinkle et
 129 al. (2018) for hurricane landfalls from 1988–2017, while damage estimates for the ten CONUS
 130 landfalling hurricanes from 2018–2020 are taken from the National Hurricane Center best track
 131 reports on these storms (<https://www.nhc.noaa.gov/data/tcr/>). Normalized damage estimates from
 132 Weinkle et al. (2018) are provided in 2018 USD, while damage estimates from the hurricane
 133 landfalls of 2018–2020 are listed in USD of the year that they made landfall. Changes in
 134 inflation, population and exposure should be relatively minor factors from 2018–2020.

135 Multiple landfalls from the same hurricane are identified if there were two separate damage
 136 estimates recorded in the Weinkle et al. (2018) dataset. From 1988–2017, three hurricanes were
 137 recorded with two separate damage estimates: Andrew (1992), Erin (1995), and Georges (1998).
 138 The results would not change significantly if only one landfall per storm were considered. None
 139 of the ten CONUS landfalling hurricanes in 2018–2020 made multiple landfalls, defined in
 140 Klotzbach et al. (2018) and here to be two separate CONUS hurricane landfalls with at least 100
 141 miles of open ocean between landfalls.

142 Integrated kinetic energy is defined as:

$$143 \quad IKE = \int_0^{2\pi} \int_0^{r_0} \frac{1}{2} \rho h V^2 r dr d\theta \quad (1)$$

144 where r is radius, V is total wind speed, ρ is near-surface air density, and h is a fluid depth. The
 145 latter two may be assumed constant and so are not important for our analysis. We estimate IKE
 146 following the methodology of Misra et al. (2013), which sets $\rho=1 \text{ kg m}^{-3}$ and $h=1 \text{ m}$ and then
 147 uses the estimates of the radius of maximum wind (R_{\max}) and the four quadrant estimates of the
 148 radius of 34-kt wind ($R_{34\text{kt}}$), radius of 50-kt wind ($R_{50\text{kt}}$) and radius of 64-kt wind ($R_{64\text{kt}}$) from
 149 the Extended Best Track. The method calculates the area within each quadrant between each pair
 150 of adjacent wind radii and uses a representative wind speed between the bounding wind speeds.
 151 IKE is then summed across all quadrant sub-regions. The algorithm is summarized in Table S1,
 152 which is identical to Table A1 of Misra et al. (2013), with one minor modification to clarify the
 153 criteria within the hurricane-force wind region (Misra personal communication. 2021–06–23).
 154 Approximately 1% of 6-hourly periods in the extended best track are excluded (all prior to 2003)
 155 either due to lack of radius of maximum winds or 34-kt wind radii which is necessary to
 156 calculate IKE.

157 Integrated kinetic energy at landfall was calculated as the IKE at the six-hourly period between
 158 12–18 hours prior to landfall, since the wind radii necessary to calculate IKE are only given
 159 at six-hourly intervals recorded in the best track (e.g., 0, 6, 12, 18 UTC). Integrated kinetic
 160 energy at this time period had slightly higher correlations with V_{\max} , MSLP and normalized
 161 damage than adjacent six-hour periods. As a hurricane gets closer to landfall, the outer
 162 circulation of the storm is already on land, likely causing deformation of the hurricane wind
 163 field. If different time periods were used to calculate landfalling IKE, the results would only
 164 change slightly.

165 We also compare results using IKE to those using power dissipation (PD; Bister & Emanuel,
 166 1998). Power dissipation scales identically with IKE except with the wind speed cubed rather
 167 than squared, and is given by:

$$168 \quad PD = \int_0^{2\pi} \int_0^{r_0} \rho C_d V^3 r dr d\theta \quad (2)$$

169
 170 where ρ is near-surface air density and C_d is the surface drag coefficient, each of which may be
 171 taken as approximately constant and so are not important for our analysis. Here we set $\rho =$
 172 1 kg/m^3 and $C_d = 10^{-3}$. We calculate PD following the same methodology as IKE above, but
 173 cubing rather than squaring the wind speed.
 174

175 Rank correlations (r_{rank}) are used as the predominant agreement metric between time series
 176 throughout the manuscript, in order to remove the influence of large outlying events (e.g.,
 177 Katrina for normalized damage or Sandy for IKE). Higher ranks are defined to be higher V_{max} ,
 178 lower MSLP (e.g., deeper storms), higher IKE and increased damage. We find that MSLP is a
 179 consistently better predictor of historical damage than both V_{max} and IKE, and we discuss the
 180 implications of this result given that MSLP is inherently an integrated measure of the wind field
 181 whose estimation is straightforward and already routinely measured.

182 Statistical significance is primarily calculated using bootstrap resampling methods and is
 183 reported at the 5% level (Efron, 1979; Hesterberg et al., 2003). Statistical significance of
 184 correlations are calculated by resampling with replacement 1000 times from the dataset being
 185 investigated. If fewer than 5% of the randomly resampled correlations are less than zero, the
 186 correlation is said to be significant. Statistical significance of correlation differences is calculated
 187 using the Fisher r to z transformation and accounting for the correlation between the two time
 188 series (Lee & Preacher, 2013).

189 **3 Relationships between V_{max} , MSLP and IKE**

190 **3.1 Full Atlantic basin**

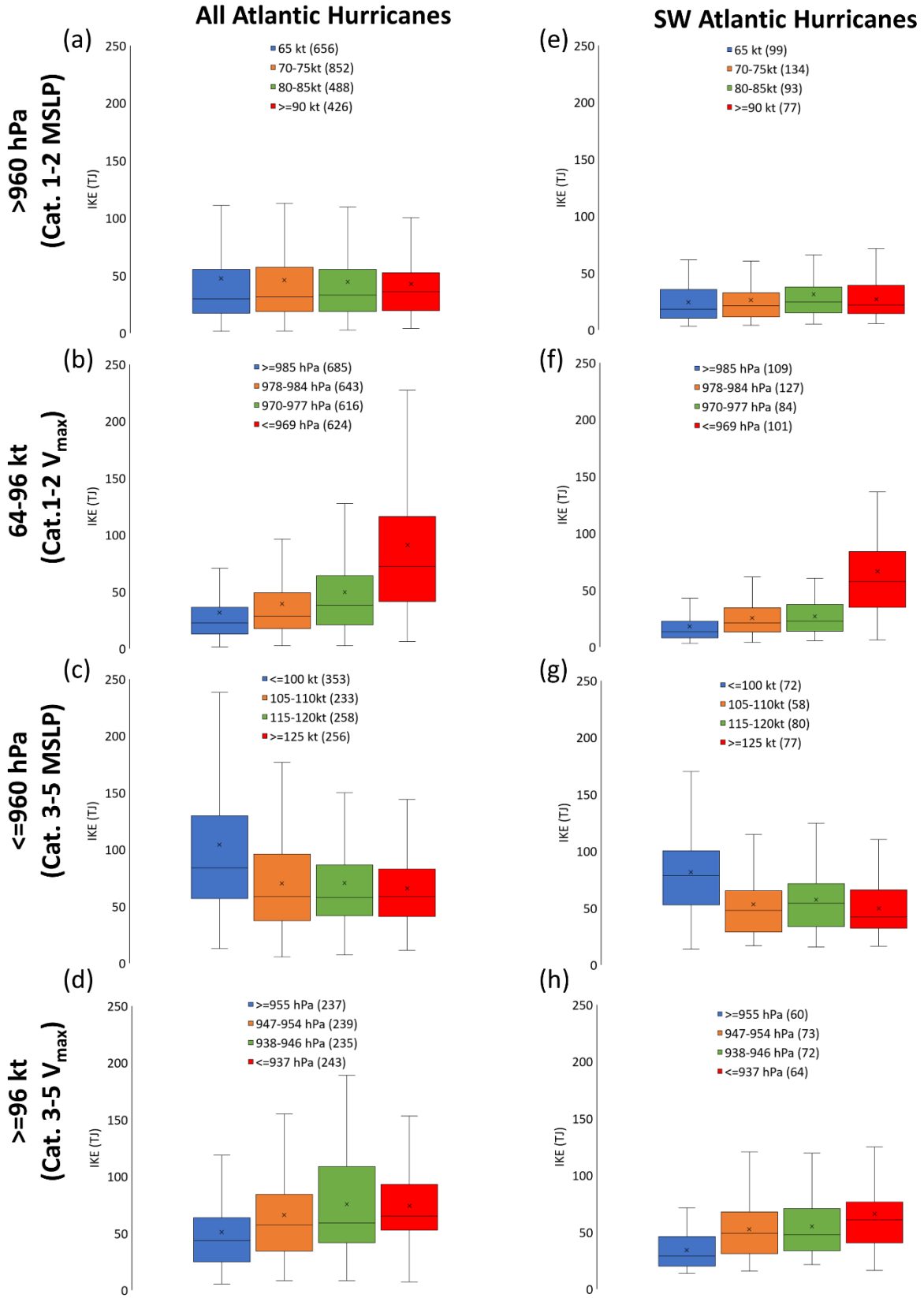
191 We begin by investigating the relationship between MSLP, V_{max} , and IKE for all Atlantic
 192 hurricanes from 1988–2020 and find that IKE covaries strongly with MSLP but not
 193 V_{max} . Overall, for all Atlantic hurricanes, the correlation between MSLP and IKE is significantly
 194 stronger ($r_{rank} = 0.50$) than between V_{max} and IKE ($r_{rank} = 0.26$).

195 We visualize this closer relationship between MSLP and IKE for both Category 1–2 hurricanes
 196 and major (Category 3–5) hurricanes in Figure 1. Figure 1a displays a boxplot of IKE for the
 197 approximate quartiles of V_{max} for Atlantic hurricanes¹ classified as Category 1–2 based on
 198 MSLP, using the Klotzbach et al. (2020) definition (e.g., >960 hPa). There is no systematic
 199 variation in IKE across quartiles of V_{max} (Figure 1a), indicating that V_{max} provides little
 200 additional information about IKE beyond what is provided by MSLP.

201 In contrast, if we take Category 1–2 hurricanes by V_{max} (e.g., 64–95 kt) and plot quartiles of
 202 MSLP (Figure 1b), there is a pronounced trend towards larger IKE values at higher pressure
 203 intensity (i.e., lower MSLP). For example, mean IKE for the strongest quartile of MSLP (≤ 969
 204 hPa) is three times larger than for the weakest quartile of MSLP (≥ 986 hPa).

205 Results are similar for major hurricanes defined by MSLP (≤ 960 hPa) and V_{max} (≥ 96 kt). V_{max}
 206 generally shows a weak relationship with IKE (Figure 1c), whereas lower MSLP generally is
 207 associated with larger values of IKE (Figure 1d).

¹Atlantic hurricanes are classified in 5 kt increments, which precludes a more precise stratification by quartiles. For example, 27% of all 6-hr periods for Category 1–2 hurricanes classified by MSLP are 65 kt, 18% are 70 kt, 17% are 75 kt, 11% are 80 kt, 8% are 85 kt, while hurricanes with $V_{max} \geq 90$ kt comprise the remaining 19% of the sample. The closest to a quartile breakdown that we can make is: 65 kt (27%), 70–75 kt (35%), 80–85 kt (19%) and ≥ 90 kt (19%)



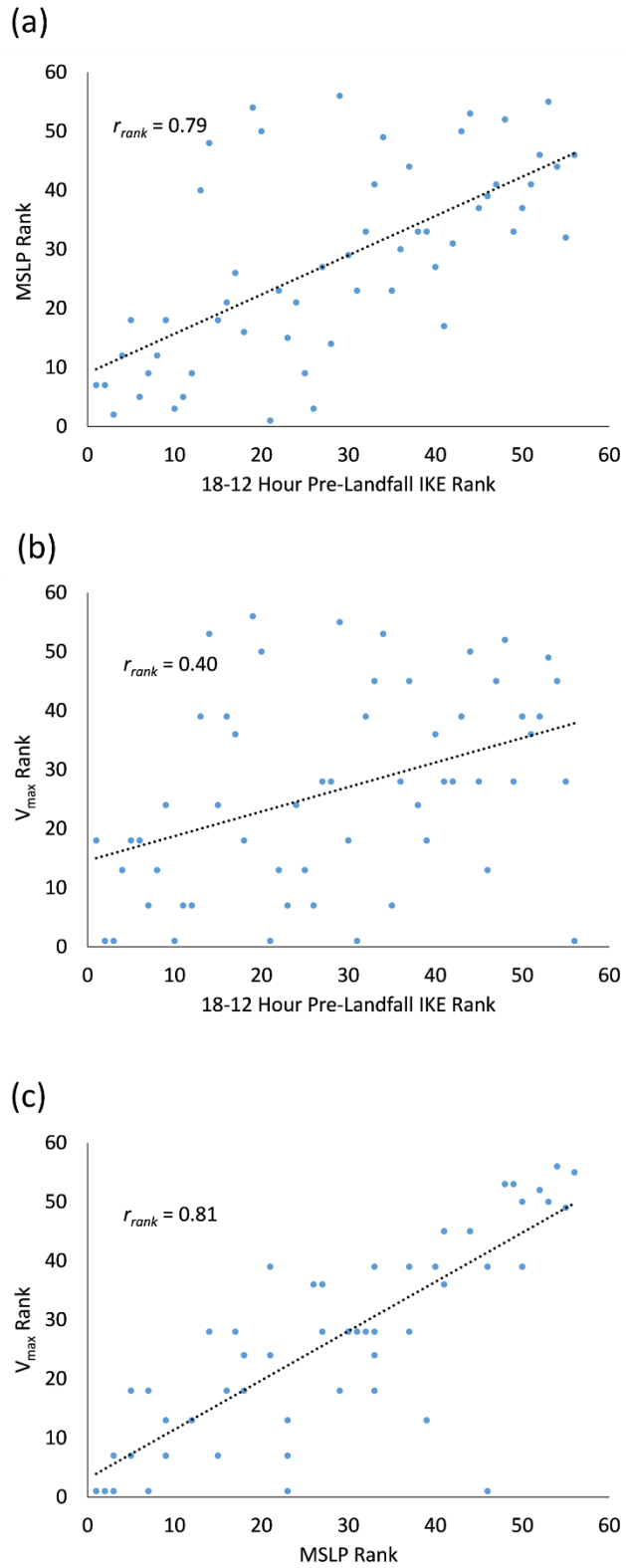
209 **Figure 1.** Quartile box plots showing relationships between MSLP, V_{\max} , and IKE for Atlantic
210 hurricanes. (a) Box plot of IKE for approximate quartiles of V_{\max} for all Atlantic Category 1–2
211 hurricanes as classified by MSLP from 1988–2020. Numbers in parentheses represent the
212 number of six-hourly hurricane observations in each quartile. (b) As in panel a but for Category
213 1–2 hurricanes classified by V_{\max} . (c) As in panel a but for all Atlantic major hurricanes
214 classified by MSLP from 1988–2020. (d) As in panel a but for all Atlantic major hurricanes
215 classified by V_{\max} from 1988–2020. (e–h) As in panels a–d but for southwest Atlantic hurricanes
216 from 2004–2020. The middle line in all box plots represents the median value, while the ‘x’ in
217 all box plots represents the mean value.

218 **3.2 Southwest Atlantic hurricanes**

219 Our results are similar when focusing on the subset of cases from the Extended Best Track
220 dataset from the southwest Atlantic Ocean since 2004 that are expected to be well-sampled by
221 aircraft (Figures 1e–h). The correlation between MSLP and IKE in the subset of the best sampled
222 cases is stronger ($r_{\text{rank}} = 0.63$) than it was for the entire Atlantic basin over the longer record, and
223 it remains significantly stronger than between V_{\max} and IKE ($r_{\text{rank}} = 0.45$). For Category 1–2
224 hurricanes, IKE again shows little systematic variation with V_{\max} (Figures 1e and 1g), while
225 systematically increasing with decreasing MSLP (Figures 1f and 1h).

226 **3.3 Continental United States landfalling hurricanes**

227 We next show that these relationships extend specifically to CONUS landfalling hurricanes at
228 landfall. Figures 2a–2c display scatterplots of the relationship between MSLP and IKE, V_{\max} and
229 IKE, and V_{\max} and MSLP, respectively, for CONUS landfalling hurricanes. As was the case for
230 basinwide hurricanes, there is a significantly stronger relationship between MSLP and IKE (r_{rank}
231 $= 0.79$) than between V_{\max} and IKE ($r_{\text{rank}} = 0.40$) for CONUS landfalling hurricanes.



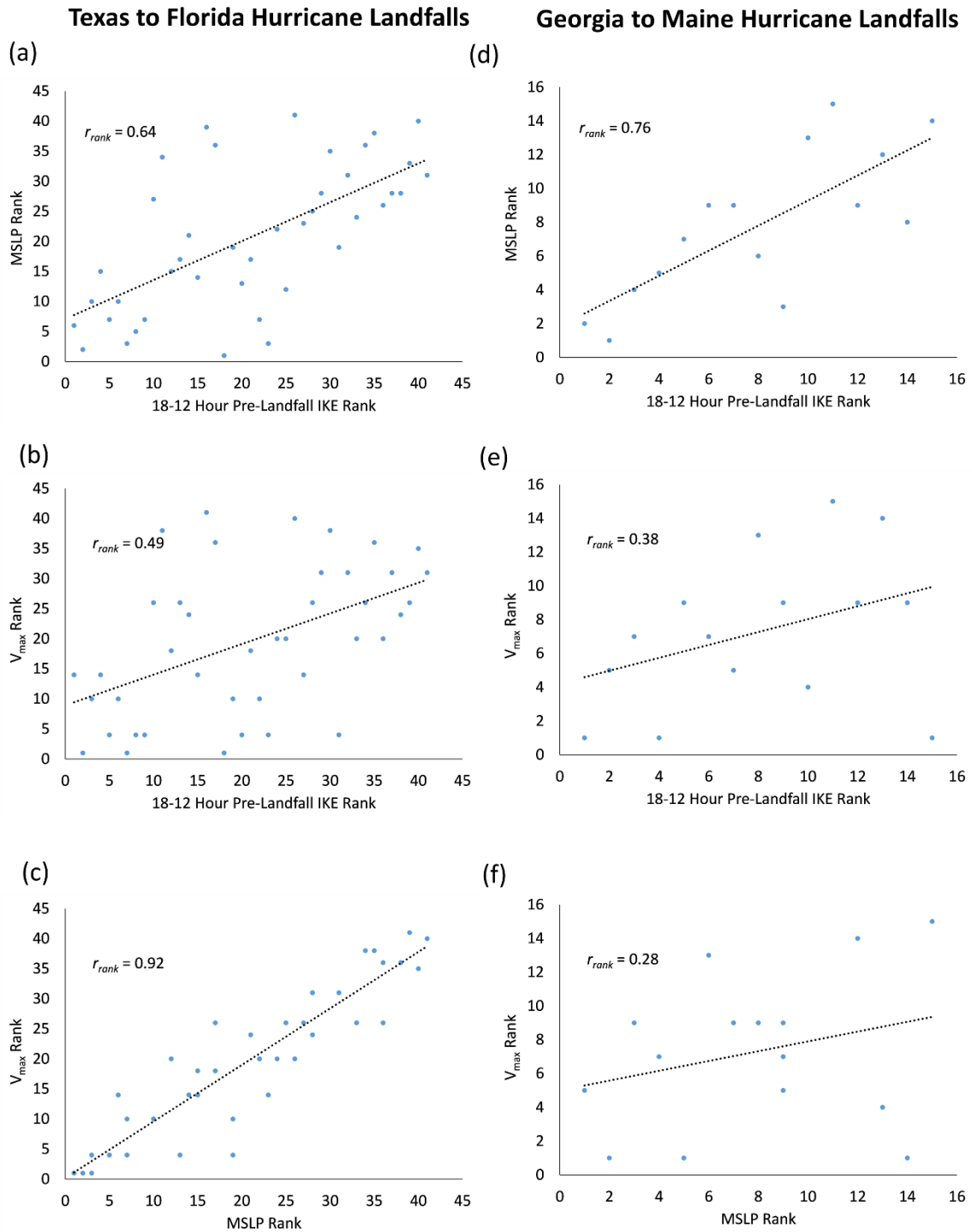
232

233 **Figure 2.** Relationship between MSLP, V_{max} and IKE for CONUS landfalling hurricanes from
 234 1988–2020. (a) Rank scatterplot of MSLP and IKE for CONUS landfalling hurricanes. (b) As in
 235 panel a but for V_{max} and IKE. (c) As in panel a but for V_{max} and MSLP.

236 3.4 Texas to Florida vs. Georgia to Maine landfalling hurricanes

237 Results are similar when we decompose landfalls by region for Texas to Florida landfalls and
238 Georgia to Maine landfalls. For Texas to Florida landfalls (Figures 3a–3c) the correlation
239 between MSLP and IKE ($r_{\text{rank}} = 0.64$) is greater than the correlation between V_{max} and IKE (r_{rank}
240 $= 0.49$). For Georgia to Maine landfalls (Figures 3d–3f) the correlation between MSLP and IKE
241 ($r_{\text{rank}} = 0.76$) is again greater than the correlation between V_{max} and IKE ($r_{\text{rank}} = 0.38$), which is a
242 starker contrast between MSLP and V_{max} than for Texas to Florida landfalls. While the
243 relationship between V_{max} and MSLP is significant and strong for Texas to Florida landfalls
244 ($r_{\text{rank}} = 0.92$), the correlation is weak and insignificant for Georgia to Maine landfalls ($r_{\text{rank}} =$
245 0.28). Hurricanes tend to grow in size as they move poleward (Knaff et al. 2014, Chavas et al.
246 2016, Klotzbach et al. 2020, Chavas and Knaff 2022), and have a larger radius of maximum
247 wind as a result (Chavas and Knaff 2022), which increases variations in IKE that may be
248 captured by MSLP but not V_{max} .

249



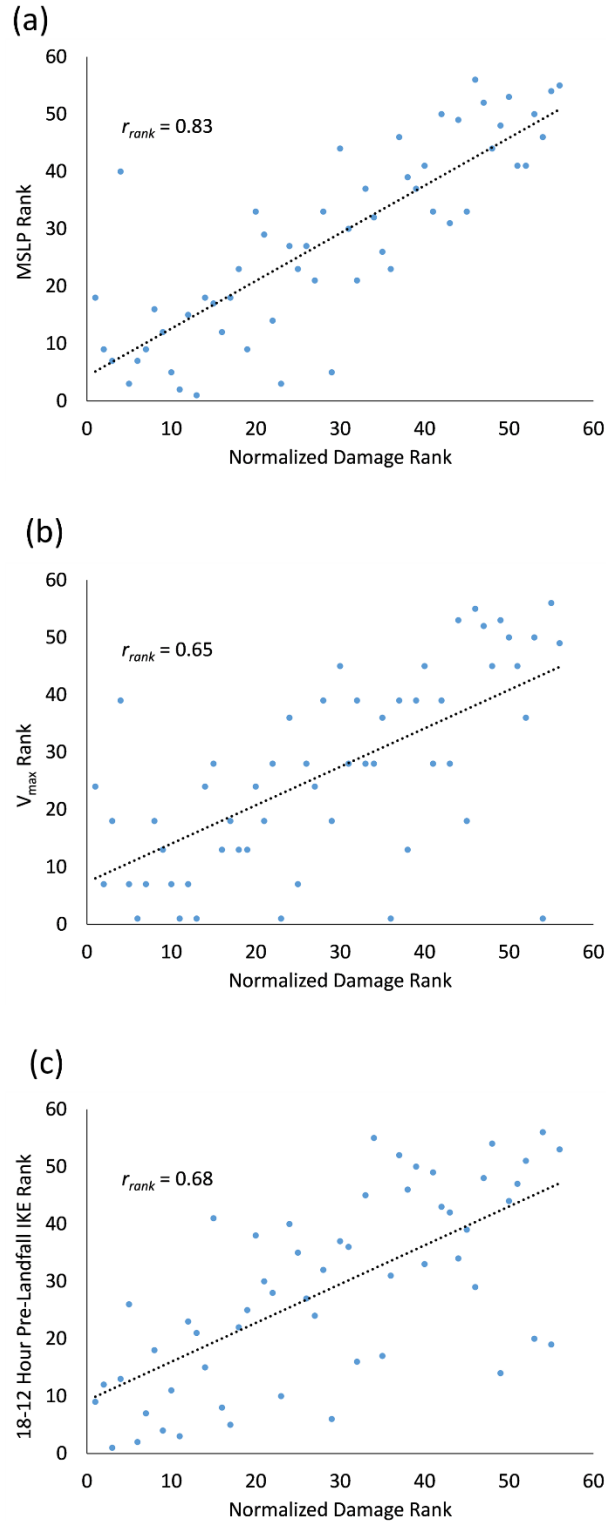
250

251 **Figure 3.** Relationship between MSLP, V_{max} and IKE for Texas to Florida landfalling hurricanes
 252 (left column) and Georgia to Maine landfalling hurricanes (right column) from 1988–2020. (a)
 253 Rank scatterplot of MSLP and IKE for Texas to Florida landfalling hurricanes. (b) As in panel a
 254 but for V_{max} and IKE. (c) As in panel a but for V_{max} and MSLP. (d–f) As in a–c but for Georgia
 255 to Maine landfalling hurricanes.

256 **4 Relationship between intensity metrics and normalized landfalling hurricane damage**

257 **4.1 Continental United States normalized landfalling hurricane damage**

258 We now show that MSLP better predicts historical damage as compared to IKE or V_{\max} ,
259 beginning with the entire US coastline. Figures 4a–c display relationships between MSLP, V_{\max}
260 and IKE with CONUS normalized damage, with higher ranks indicating stronger storms and
261 increased damage. The correlation between MSLP and CONUS normalized damage ($r_{\text{rank}} =$
262 0.83; Figure 4a) is significantly stronger (as highlighted by the stronger slope of the best fit line)
263 than the correlation between V_{\max} and CONUS normalized damage ($r_{\text{rank}} = 0.65$; Figure 4b). The
264 MSLP-CONUS normalized damage correlation is also significantly stronger than the correlation
265 between IKE and CONUS normalized damage ($r_{\text{rank}} = 0.68$; Figure 4c).



266

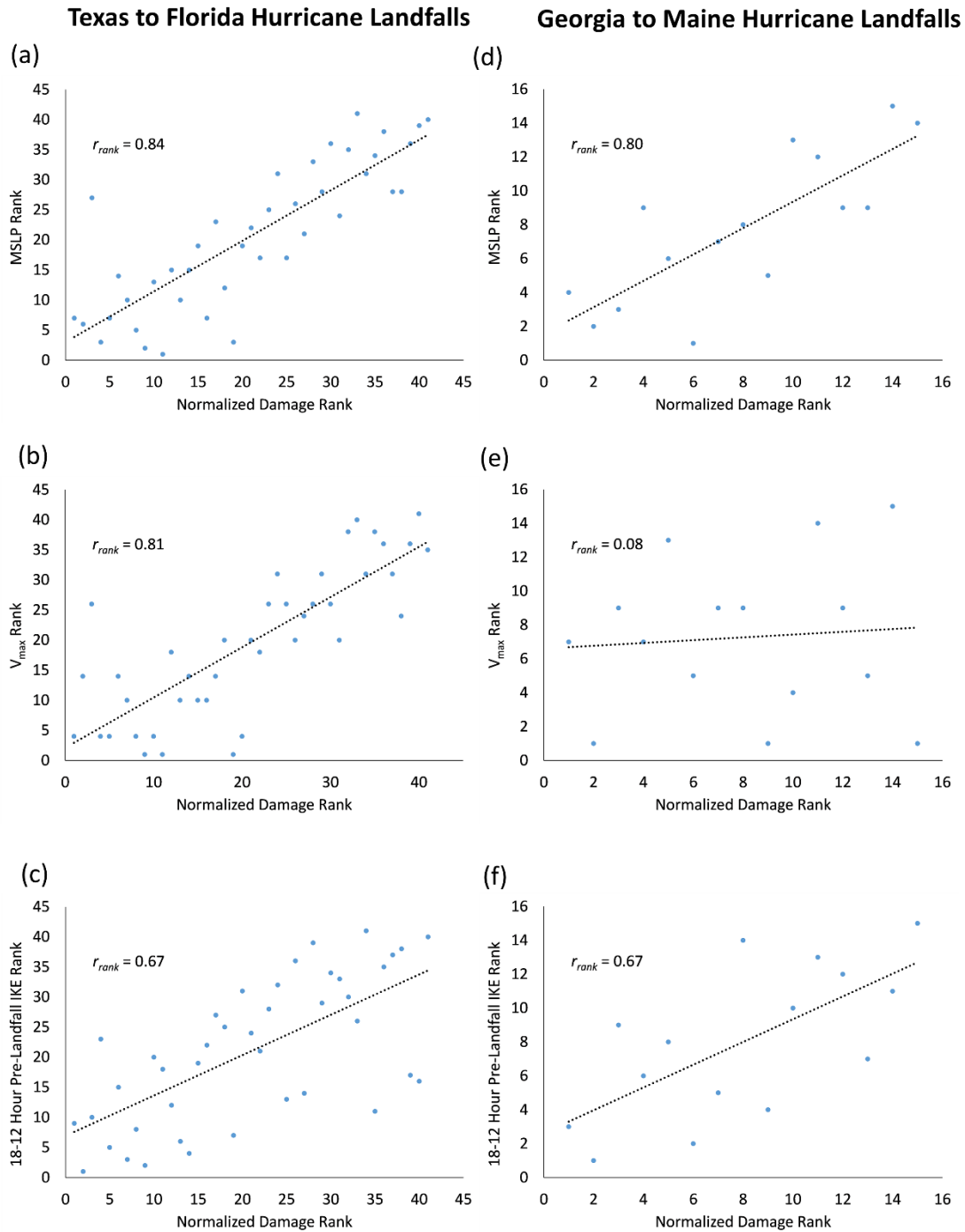
267 **Figure 4.** Relationship between intensity metrics and CONUS landfalling hurricane damage
268 from 1988–2020. (a) Rank scatterplot of MSLP and damage from CONUS landfalling
269 hurricanes. (b) As in panel a but for V_{max} and damage from CONUS landfalling hurricanes. (c)
270 As in panel a but for IKE and damage from CONUS landfalling hurricanes.

271 4.2 Texas to Florida vs. Georgia to Maine normalized landfalling hurricane damage

272 Klotzbach et al. (2020) noted similar correlations for Texas to Florida hurricane landfalls
273 between V_{\max} and normalized damage as between MSLP and normalized damage, while MSLP
274 was a much more skillful predictor of damage than V_{\max} for Georgia to Maine hurricane
275 landfalls. We now show that MSLP is also a better predictor for these two regions compared to
276 both IKE and V_{\max} , particularly for Georgia to Maine.

277 For Texas to Florida landfalls, the correlation between MSLP and normalized damage ($r_{\text{rank}} =$
278 0.84 ; Figure 5a) and V_{\max} and normalized damage ($r_{\text{rank}} = 0.81$; Figure 5b) are both strong and
279 nearly equal. Meanwhile, the correlation between IKE and normalized damage is slightly weaker
280 ($r_{\text{rank}} = 0.67$; Figure 5c). These results for the relationship between both V_{\max} and MSLP with
281 normalized damage are similar to that of Klotzbach et al. (2020).

282 For Georgia to Maine landfalls, the correlation between MSLP and normalized damage is strong
283 ($r_{\text{rank}} = 0.80$, Figure 5d). The correlation between IKE and normalized damage is a bit weaker
284 ($r_{\text{rank}} = 0.67$, Figure 5f). Both of these correlations are similar to their Texas to Florida
285 correlation values. However, the correlation between V_{\max} and normalized damage is extremely
286 weak ($r_{\text{rank}} = 0.08$, Figure 5e) and is not significant. Hence, hurricane metrics that either
287 explicitly (IKE) or implicitly (MSLP) have a size component are more skillful for hurricanes
288 making landfall along the East Coast of the United States north of Florida. This result for
289 damage aligns with the finding above that V_{\max} itself is poorly correlated with IKE for this
290 landfall region ($r_{\text{rank}} = 0.38$, Figure 3e).



291

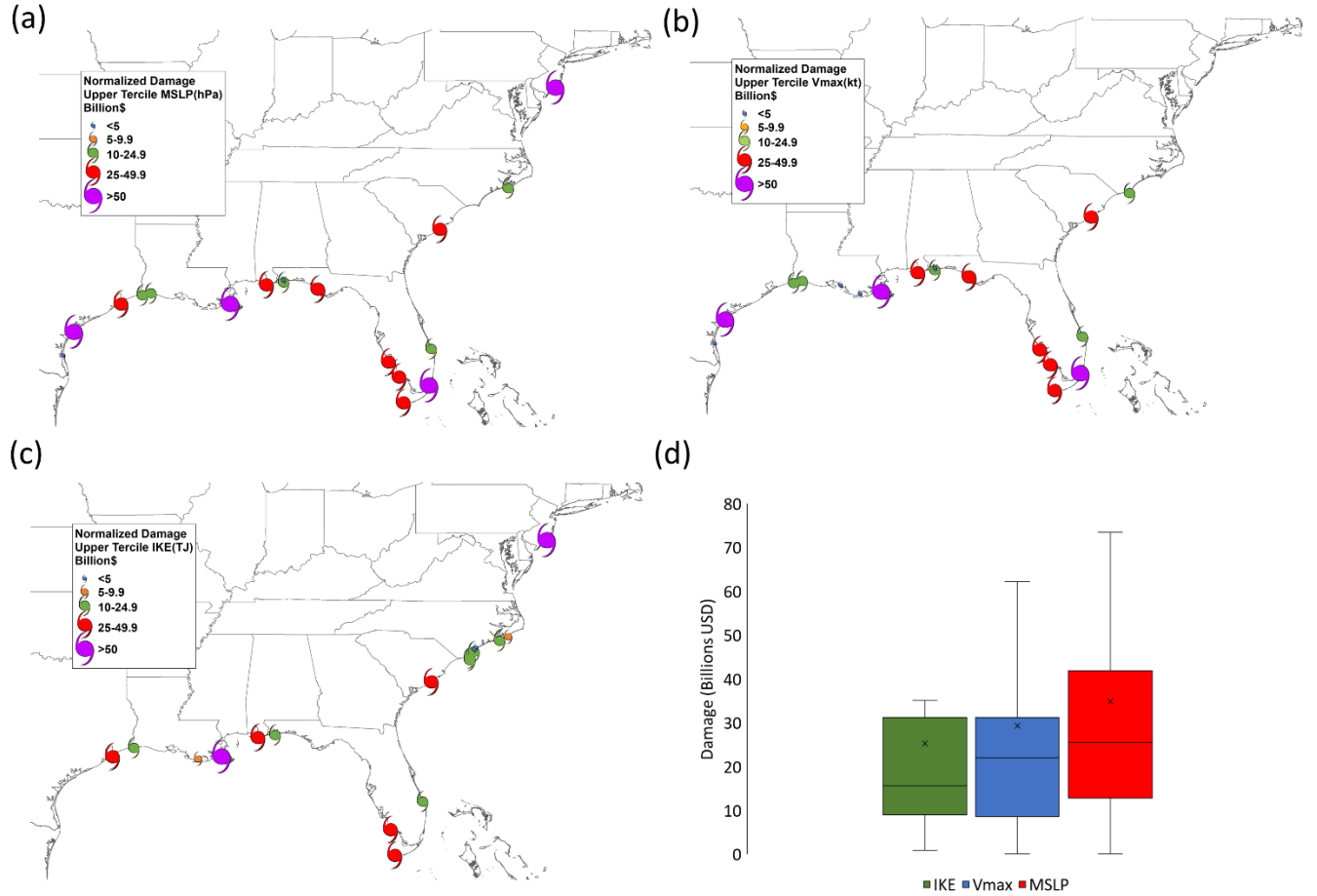
292 **Figure 5.** Relationship between MSLP, V_{max} and IKE with normalized damage for Texas to
 293 Florida landfalling hurricanes (left column) and Georgia to Maine landfalling hurricanes (right
 294 column) from 1988–2020. (a) Rank scatterplot of MSLP and normalized damage for Texas to
 295 Florida landfalling hurricanes. (b) As in panel a but for V_{max} and normalized damage for Texas
 296 to Florida landfalling hurricanes. (c) As in panel a but for IKE and normalized damage for Texas
 297 to Florida landfalling hurricanes. (d–f) As in a–c but for Georgia to Maine landfalling hurricanes.

298 A prime example of this is Sandy (2012), whose V_{\max} was barely at hurricane-equivalent
299 intensity at landfall yet had a very low MSLP owing in part to its exceptionally large size
300 (Halverson & Rabenhorst 2013; Chavas et al. 2018). We note that the correlation between V_{\max}
301 and normalized damage for Georgia to Maine is considerably lower than what was found in
302 Klotzbach et al. (2020) from 1900–2018 ($r_{\text{rank}} = 0.42$). The degradation in the correlation is due
303 to a relatively smaller sample size of Georgia to Maine hurricane landfalls from 1988–2020 (e.g.,
304 15 landfalls) that also includes Sandy. One outlier in a small sample can considerably impact a
305 correlation value. If Sandy were excluded from the 1988–2020 analysis, the correlation between
306 V_{\max} and normalized damage for Georgia to Maine would remain insignificant ($r_{\text{rank}} = 0.29$) but
307 would be more in line with the correlation reported in Klotzbach et al. (2020).

308 **4.3 Upper tercile of continental US landfalling hurricane damage**

309 As an alternative way of demonstrating the value of MSLP as a damage predictor, we show that
310 the historical damage caused by the strongest storms is systematically higher when storm
311 strength is defined by MSLP. From 1988–2020, 18 hurricanes made landfall in the CONUS with
312 a maximum intensity of 100 kt or greater - Category 3+ on the Saffir–Simpson Hurricane Wind
313 Scale. Given that 56 CONUS landfalling hurricanes occurred from 1988–2020, this equates to
314 the approximate upper tercile of landfalling hurricanes during the 33-year period. Figures 6a–c
315 display the location of the 18 strongest landfalling hurricanes using MSLP (≤ 952 hPa), V_{\max}
316 (≥ 100 kt) and IKE (≥ 71 TJ) criteria. While the spatial distribution of the upper tercile using
317 MSLP (Figure 6a) and V_{\max} (Figure 6b) is similar, many more hurricanes from Georgia to Maine
318 classify as upper tercile storms using IKE (Figures 6c). Using V_{\max} , two hurricanes from Georgia
319 to Maine are in the upper tercile (Hugo (1989) and Fran (1996)). Using MSLP, in addition to
320 Hugo and Fran, Sandy (2012) also is in the upper tercile. Using IKE, half of the 18 hurricanes in
321 the upper tercile made landfall from Georgia to Maine. The larger number of high-IKE landfalls
322 from Georgia to Maine is likely due to the growth in size of hurricanes as they move poleward
323 and the relatively strong weighting of 34-kt and 50-kt wind radii in the IKE equation (discussed
324 in more detail in the next section).

325 Finally, Figure 6d displays a box plot for normalized damage for the upper tercile of landfalling
326 hurricanes with intensity defined using MSLP, IKE, or V_{\max} . The mean, median and high
327 quantiles of normalized damage are all largest when using MSLP, second largest when using
328 IKE, and smallest when using V_{\max} . This analysis again highlights the improved relationship
329 using MSLP than either IKE or V_{\max} for representing the damage potential from hurricanes.



330

331 **Figure 6.** Location and relationship between the upper tercile of hurricane intensity categorized
 332 by MSLP, V_{max} , and IKE and normalized damage. (a) Location of upper tercile CONUS
 333 landfalling hurricanes from 1988–2020 based on MSLP with the size of the hurricane symbol
 334 proportional to the normalized damage. (b) As in panel a but for the upper tercile based on V_{max} .
 335 (c) As in panel a but for the upper tercile based on IKE. (d) Box plot showing the distribution of
 336 normalized damage for the upper tercile of CONUS landfalling hurricanes classified by IKE,
 337 V_{max} and MSLP.

338 5 Physical discussion

339 As shown above, an integral measure of the storm wind field (MSLP or IKE) is preferable to a
 340 point estimate of the maximum wind speed for predicting potential damage, with MSLP
 341 performing best. Here we show how MSLP represents a radial integral of the wind field, and
 342 how that integral weights wind speeds at different radii differently from IKE.

343

344 For an axisymmetric field, a radially-integrated quantity, X , may be written as:

345

346

$$X = \int_0^{r_0} x \, dr \quad (3)$$

347

348 where x is the integrand and r_0 is some larger radius (e.g., R_{34kt}). For ease of interpretation we
 349 may neglect multiplicative factors in each equation that may be taken as approximately constant,
 350 as we use these quantities purely as statistical predictors of damage. Thus, absolute magnitudes
 351 do not matter.

352

353 MSLP represents a reduction in pressure at the storm center relative to the ambient
 354 environmental pressure P_{env} at the outer edge of the storm. This pressure difference is commonly
 355 referred to as the central pressure deficit:

356

$$357 \quad dP = P_{env} - MSLP \quad (4)$$

358

359 and is related to the wind field via gradient wind balance (Knaff and Zehr 2007, Chavas et al
 360 2017). Hence, for dP , the integrand is given by:

361

$$362 \quad x_{dP} \sim \frac{V^2}{r} + fV \quad (5)$$

363

364 where we drop the density factor (ρ). For IKE, from Eq. (1) the integrand is given by:

365

$$366 \quad x_{IKE} \sim rV^2 \quad (6)$$

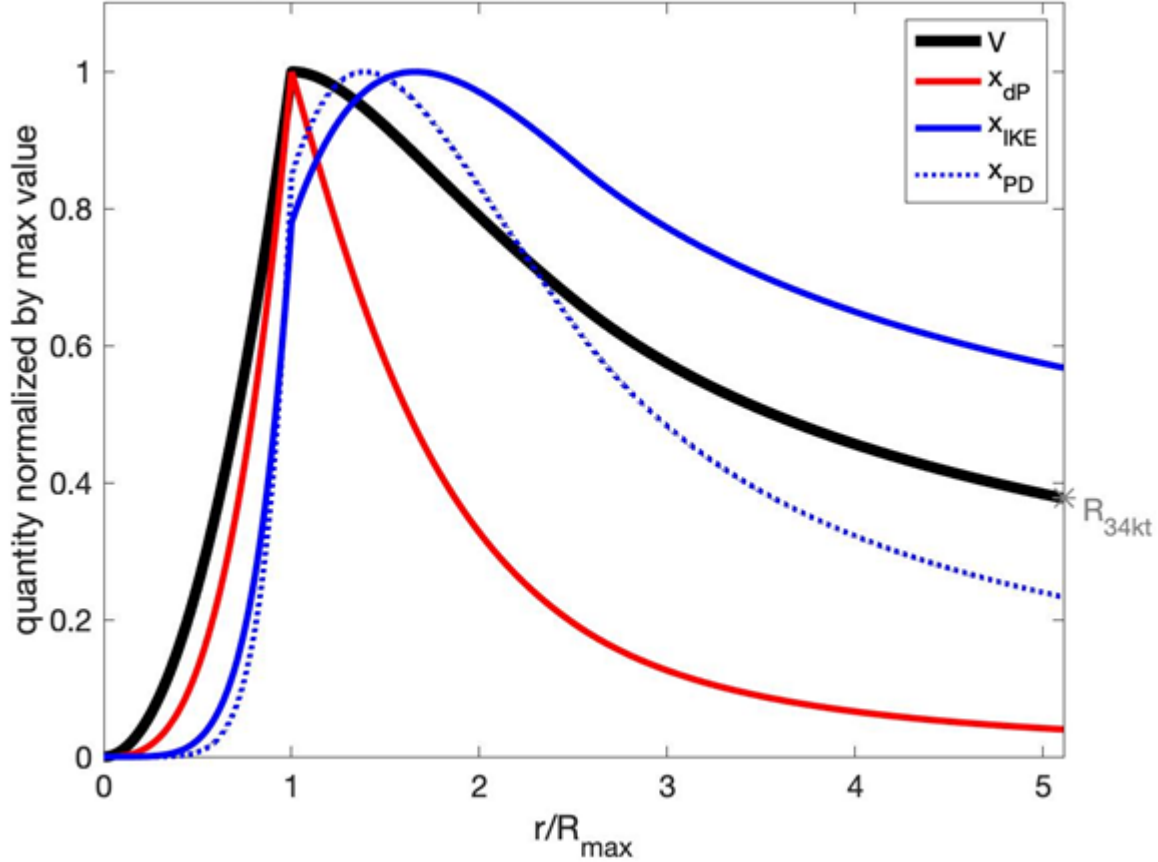
367

368 where r arises from the polar integral, and we drop the factor $\frac{1}{2}\rho h$.

369

370 To show how each quantity weights wind speeds at different radii, each integrand x may be
 371 normalized by its maximum value, and the result analyzed as a function of radius normalized by
 372 the radius of maximum wind. An example calculation is shown in Figure 7 for a characteristic
 373 hurricane wind profile defined by the model of Chavas et al. (2015). This model has been shown
 374 to capture the observed structure of the complete hurricane wind field as well as the basic
 375 structural relationships between R_{max} , R_{34kt} , and V_{max} in the historical record (Chavas and Knaff
 376 2022). For this example, the model is defined using parameter values taken as the median values
 377 of southwest Atlantic hurricanes: $R_{max} = 28$ km, $V_{max} = 90$ kt, and latitude at $23.7^\circ N$. The central
 378 pressure deficit is weighted towards the strongest wind speeds in the inner core ($r < 2R_{max}$),
 379 and its maximum weighting is at R_{max} itself. Integrated kinetic energy has a similar qualitative
 380 structure but more strongly weights weaker wind speeds at larger radii towards R_{34kt} , with its
 381 maximum value at about $1.7R_{max}$. This difference arises because V^2 is weighted inversely by
 382 radius in the centrifugal term $\frac{V^2}{r}$ in x_{dP} , and so x_{dP} decreases rapidly beyond R_{max} , whereas V^2
 383 is weighted proportionally to radius in x_{IKE} .

384



385
386

387 **Figure 7.** Radial structure of the pressure deficit (dP; red), integrated kinetic energy (IKE; blue),
388 and power dissipation (PD; cyan) calculated from an example tropical cyclone wind profile (V;
389 black). Each quantity is normalized by its maximum value, and radius is normalized by the
390 radius of maximum wind, R_{\max} . The wind profile is defined using the physical model of Chavas
391 et al. (2015) taking as input the median values of southwest Atlantic hurricanes: $V_{\max} = 90$ kt,
392 $R_{\max} = 28$ km, and latitude at 23.7°N . A simple quadratic profile is used in the eye for $r < R_{\max}$.
393 $R_{34\text{kt}}$ is marked with a gray star. Each colored curve represents the integrand whose radial
394 integral scales with the given quantity. This quantity is normalized by its maximum value to
395 allow for direct comparison across dP, IKE, and PD (see text for details).

396

397 A viable alternative integral quantity to IKE is PD. Power dissipation scales identically with IKE
398 except with the wind speed cubed rather than squared. While IKE (units of Joules) is much more
399 widely used, PD (units of Watts) has physical appeal for damage potential because it represents
400 the rate of transfer of kinetic energy from the near-surface air into the surface due to surface
401 friction. For PD, from Eq. (2) the integrand is given by:

402

$$403 \quad x_{PD} \sim rV^3 \quad (7)$$

404

405 where r again arises from the polar integral, and we drop the factor ρC_d . Power dissipation
406 yields a weighting of the radial structure that lies in between dP and IKE (Figure 7). This
407 behavior arises because V^3 more strongly weights higher wind speeds than V^2 .

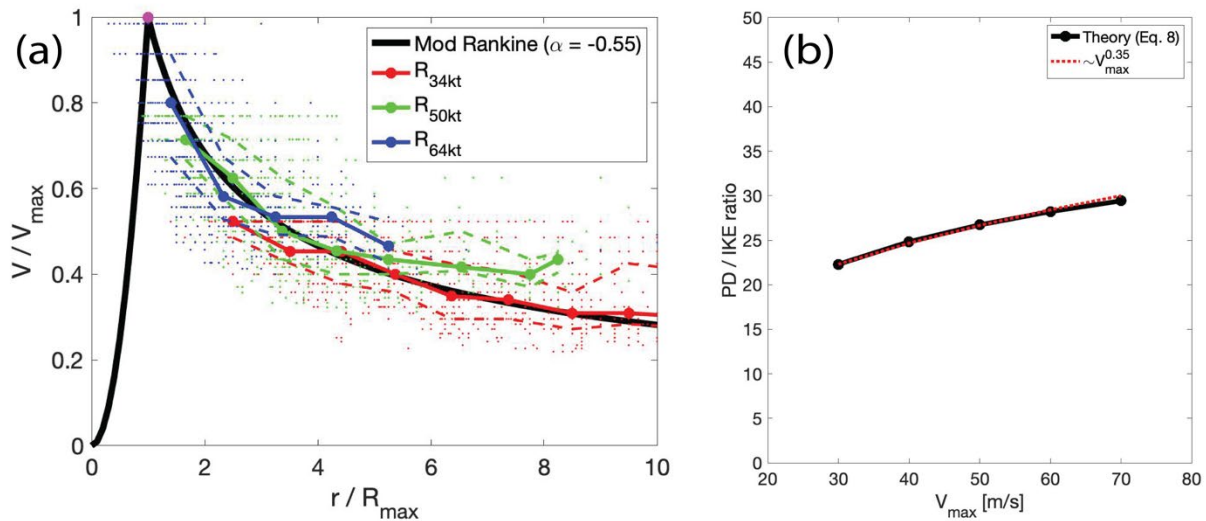
408

409 However, our results are nearly identical when applying our methodology for PD rather than
 410 IKE. Despite their different weighting structures, variations in PD and IKE correlate very
 411 strongly with one another ($r_{\text{rank}} = 0.99$; Figure S1). The close relationship between IKE and PD
 412 arises because the inner wind field is well-approximated by a Modified Rankine vortex (Rappin
 413 et al. 2013), given by $\tilde{V} = \tilde{r}^\alpha$, where $\tilde{r} = r/R_{\text{max}}$ and $\tilde{V} = V/V_{\text{max}}$. The statistics of the
 414 Extended Best Track wind radii data maps closely onto a Rankine vortex with an exponent $\alpha =$
 415 -0.55 (Figure 8a). For this wind profile solution, the ratio of PD to IKE between R_{max} and $R_{34\text{kt}}$
 416 can be derived analytically, and may be written as:

$$418 \quad \frac{\text{PD}}{\text{IKE}} \sim \left(\frac{2\alpha+2}{3\alpha+2} \right) V_{\text{max}} \left(\frac{\tilde{V}_{34\text{kt}}^{3+\frac{2}{\alpha}} - 1}{\tilde{V}_{34\text{kt}}^{2+\frac{2}{\alpha}} - 1} \right) \quad (8)$$

419 where $\tilde{V}_{34\text{kt}} = V_{34\text{kt}}/V_{\text{max}}$, $V_{34\text{kt}}$ is simply the gale force wind speed, and we have neglected the
 420 constants in each quantity as described above. This solution neglects winds within the eye
 421 ($r < R_{\text{max}}$). Eq. 8 shows that, for fixed values of α and wind speed of the bounding radius ($V_{34\text{kt}}$),
 422 the ratio of PD to IKE depends only on V_{max} ; it does not depend on R_{max} . Moreover, the
 423 dependence on V_{max} is weak (Figure 8b), following a scaling of approximately $V_{\text{max}}^{0.35}$. As a
 424 result, IKE and PD scale very closely together and are nearly equivalent as predictors for
 425 historical damage. A more detailed analysis of the relationship between IKE and PD in observed
 426 storms may be an interesting avenue for future research.

427



428 **Figure 8.** (a) Statistics of Extended Best Track wind radii ($R_{34\text{kt}}$ in blue, $R_{50\text{kt}}$ in green, $R_{64\text{kt}}$
 429 in red) plotted with radius normalized by the radius of maximum wind speed and wind speed
 430 normalized by maximum wind speed, for the 2004-2020 southwest Atlantic subset. Median
 431 (solid) and interquartile range (dashed; 25th-75th percentile) values of $(r/R_{\text{max}}, V/V_{\text{max}})$
 432 calculated within unit bins of r/R_{max} (i.e. 1-2, 2-3, etc.); values plotted in bins with at least 10
 433 datapoints. Modified Rankine profile shown (black) with $\alpha = -0.55$. (b) Ratio of PD to IKE for
 434 the Modified Rankine solution between R_{max} and $R_{34\text{kt}}$ (Eq. 8) as a function of V_{max} (black),
 435 with approximate scaling (red) for comparison.

437
438 Note that technically the weighted-average wind speeds (Table S1) should be recalculated for
439 V^3 , but doing so using a piecewise-linear model of the wind field has a negligible change to this
440 outcome (not shown).

441
442 Ultimately there is likely no single “correct” weighting of the radial structure when relating the
443 wind field to damage potential, as storm hazards (wind, surge, and rainfall) each depend on
444 different aspects of the wind field in addition to an array of other environmental factors that can
445 vary from storm to storm. Indeed, our results indicate that IKE and PD are equally useful as
446 predictors of damage potential despite their different weighting structures. We find that MSLP is
447 slightly more useful as a damage predictor, suggesting that its weighting structure may be better
448 suited for representing damage potential or other direct/indirect societal disruptions.
449 Explanations for why that might be are highly complex, though, and hence we leave this topic
450 for future work.

451 **6 Summary and conclusions**

452 Here we have investigated the relationship between IKE, V_{\max} and MSLP for both Atlantic basin
453 hurricanes and for CONUS landfalling hurricanes, specifically from 1988–2020. We find that
454 IKE has a stronger relationship with MSLP than with V_{\max} , both for basinwide hurricanes and
455 CONUS landfalling hurricanes. This finding is likely due to the robust relationship between
456 storm size and central pressure deficit, as the central pressure is itself an integrated measure of
457 the wind field. When focusing specifically on well-measured southwest Atlantic hurricanes and
458 using rank correlations, V_{\max} explains ~25% of the variance in IKE, while MSLP explains ~40%
459 of the variance in IKE.

460 Minimum sea level pressure is a better predictor of CONUS landfalling hurricane damage than
461 IKE and especially V_{\max} . While all three metrics show strong skillful correlations for hurricanes
462 making landfall from Texas to Florida, the correlation between V_{\max} and landfalling hurricane
463 damage is small and insignificant for hurricanes making landfall from Georgia to Maine. The
464 degradation in the relationship between V_{\max} and normalized damage for hurricanes making
465 landfall along the East Coast of the United States north of Florida is likely due to the growth in
466 size of hurricanes as they move poleward. Hence, our analysis indicates that the use of MSLP to
467 categorize hurricane strength would have especially high value for potential landfalls along the
468 East Coast. Very similar results are obtained when using PD as an integrated wind field quantity
469 as opposed to IKE because the wind profile is well-approximated by a Modified Rankine profile,
470 for which the two quantities scale closely with each other.

471
472 Importantly, an additional benefit of using MSLP to categorize hurricanes is that it is already
473 routinely measured operationally. Furthermore, it is much simpler to estimate than either the full
474 hurricane wind field or even V_{\max} given its relatively noisy nature. In essence, MSLP is a storm-
475 integrated quantity that can be measured directly (in principle) at a single point at the center of
476 the storm. In contrast, IKE requires estimating the wind field over a large range of radii along
477 multiple azimuths. Since MSLP is found to be the best predictor of historical hurricane damage
478 and is relatively easy to measure, we conclude that MSLP is an ideal metric for categorizing
479 damage potential for hurricanes. Based on these findings, we advocate for efforts to improve

480 forecasts and interpretation of MSLP as an intensity metric when communicating tropical
481 cyclone societal risk to the general public.

482 **Acknowledgments**

483 P. Klotzbach would like to acknowledge a grant from the G. Unger Vetlesen Foundation. D.
484 Chavas acknowledges NSF Grants 1826161 and 1945113. M. Bell was supported by Office of
485 Naval Research Grant N000142012069. C. Schreck was supported by NOAA through the
486 Cooperative Institute for Satellite Earth System Studies under Cooperative Agreement
487 NA19NES4320002. E. Gibney's research at the National Hurricane Center is supported by
488 NOAA's Science Collaboration Program and administered by UCAR's Cooperative Programs for
489 the Advancement of Earth System Science (CPAESS) under award NA21OAR4310383.

490 **Data Availability Statement**

491 All data used in this study are publicly available at the following locations:

492

493 *Extended Best Track:*

494

495 https://rammb2.cira.colostate.edu/research/tropical-cyclones/tc_extended_best_track_dataset/

496

497 *Continental US Hurricane Landfalls:*

498

499 https://www.aoml.noaa.gov/hrd/hurdat/UShurrs_detailed.html

500

501 *Normalized Continental US Hurricane Damage (1988–2017):*

502

503 [https://static-content.springer.com/esm/art%3A10.1038%2Fs41893-018-0165-
504 2/MediaObjects/41893_2018_165_MOESM2_ESM.xlsx](https://static-content.springer.com/esm/art%3A10.1038%2Fs41893-018-0165-2/MediaObjects/41893_2018_165_MOESM2_ESM.xlsx)

505

506 *Normalized Continental US Hurricane Damage (2018–2020):*

507

508 <https://www.nhc.noaa.gov/data/tcr/>

509 **References**

510 Bister, M. & Emanuel, K.A. (1998). Dissipative heating and hurricane intensity. *Meteorology
511 and Atmospheric Physics*, 65(3), 233–240. <https://doi.org/10.1007/BF01030791>

512 Buchanan, S., Misra, V., & Bhardwaj, A. (2018). Integrated kinetic energy of Atlantic tropical
513 cyclones in a global ocean surface wind analysis. *International Journal of Climatology*, 38(6),
514 2651–2661. <https://doi.org/10.1002/joc.5450>.

515 Chavas D .R., & Knaff, J. A. (2022). A simple model for predicting the tropical cyclone radius of
516 maximum wind from outer size. *Weather and Forecasting*, Early Online Release.

517 <https://doi.org/10.1175/WAF-D-21-0103.1>

518 Chavas, D. R., Lin, N., Dong, W., & Lin, Y. (2016). Observed tropical cyclone size revisited.

519 *Journal of Climate*, 29(8), 2923–2939. <https://doi.org/10.1175/JCLI-D-15-0731.1>

- 520 Chavas, D. R., Reed, K. A., & Knaff, J. A. (2017). Physical understanding of the tropical cyclone
521 wind-pressure relationship. *Nature Communications*, 8, 1360. [https://doi.org/10.1038/s41467-](https://doi.org/10.1038/s41467-017-01546-9)
522 [017-01546-9](https://doi.org/10.1038/s41467-017-01546-9)
- 523 Chavas D. R., Reed, K. A., & Knaff, J. A. (2018). Conference notebook: Physical understanding
524 of the tropical cyclone wind-pressure relationship. *Bulletin of the American Meteorological*
525 *Society*, 99(12), 2449.
526 https://web.ics.purdue.edu/~dchavas/download/ChavasReedKnaff2018BAMS_TCWindPressure
527 [ConferenceNotebookSandyExample.pdf](https://web.ics.purdue.edu/~dchavas/download/ChavasReedKnaff2018BAMS_TCWindPressure)
- 528 Demuth, J. L., DeMaria, M., & Knaff, J. A. (2006). Improvement of advanced microwave
529 sounding unit tropical cyclone intensity and size estimation algorithms. *Journal of Applied*
530 *Meteorology and Climatology*, 45(11), 1573–1581. <https://doi.org/10.1175/JAM2429.1>
- 531 Efron, B., (1979). Bootstrap methods: Another look at the jackknife. *The Annals of Statistics*,
532 7(1), 1–26. <https://doi.org/10.1214/aos/1176344552>
- 533 Emanuel, K.A., (1999). The power of a hurricane: An example of reckless driving on the
534 information superhighway. *WEATHER-LONDON*, 54, 107-108.
- 535 Grinsted, A., Ditlevsen, P., & Christensen, J. H. (2019). Normalized US hurricane damage
536 estimates using area of total destruction, 1900–2018. *Proceedings of the National Academy of*
537 *Sciences*, 116(48), 23942–23946. <https://doi.org/10.1073/pnas.1912277116>
- 538 Halverson, J. B., & Rabenhorst, T. (2013). Hurricane Sandy: The science and impacts of a
539 superstorm. *Weatherwise*, 66(2), 14–23. <https://doi.org/10.1080/00431672.2013.762838>
- 540 Hesterberg, T. S., Monaghan, S., Moore, D. S., Clipson, A., Epstein, R. (2003). Bootstrap
541 methods and permutation tests. Companion chapter 18 to *The Practice of Business Statistics*. W.
542 H. Freeman and Company, New York, 85 pp.
543 <https://statweb.stanford.edu/~tibs/stat315a/Supplements/bootstrap.pdf>
- 544 Irish, J. L., Resio, D. T., & Ratcliff, J. J. (2008). The influence of storm size on hurricane surge.
545 *Journal of Physical Oceanography*, 38(9), 2003–2013. <https://doi.org/10.1175/2008JPO3727.1>
- 546 Klotzbach, P. J., Bell, M. M., Bowen, S. G., Gibney, E. J., Knapp, K. R., & Schreck, C. J., III.
547 (2020). Surface pressure a more skillful predictor of normalized hurricane damage than
548 maximum sustained wind, *Bulletin of the American Meteorological Society*, 101(6), E830–E846.
549 <https://doi.org/10.1175/BAMS-D-19-0062.1>
- 550 Klotzbach, P. J., Bowen, S. G., Pielke Jr., R., & Bell, M. M. (2018). Continental United States
551 landfall frequency and associated damage: Observations and future risks. *Bulletin of the*
552 *American Meteorological Society*, 99(7), 1359–1376. [https://doi.org/10.1175/BAMS-D-17-](https://doi.org/10.1175/BAMS-D-17-0184.1)
553 [0184.1](https://doi.org/10.1175/BAMS-D-17-0184.1)
- 554 Knaff, J. A., Longmore, S. P., & Molenaar, D. A. (2014). An objective satellite-based tropical
555 cyclone size climatology. *Journal of Climate*, 27(1), 455–476. [https://doi.org/10.1175/JCLI-D-](https://doi.org/10.1175/JCLI-D-15-0610.1)
556 [15-0610.1](https://doi.org/10.1175/JCLI-D-15-0610.1)

- 557 Knaff, J. A., & Zehr, R. M. (2007). Reexamination of tropical cyclone wind-pressure
558 relationships. *Weather and Forecasting*, 22(1), 71–88. <https://doi.org/10.1175/WAF965.1>
- 559 Kozar, M. E., & Misra, V. (2014). Statistical prediction of integrated kinetic energy in North
560 Atlantic tropical cyclones. *Monthly Weather Review*, 142(12), 4646–4657.
561 <https://doi.org/10.1175/MWR-D-14-00117.1>.
- 562 Landsea, C. W., & Franklin, J. L. (2013). Atlantic hurricane database uncertainty and
563 presentation of a new database format. *Monthly Weather Review*, 141(10), 3576–3592.
564 <https://doi.org/10.1175/MWR-D-12-00254.1>
- 565 Lee, I. A., & Preacher, K. J. (2013). Calculation for the test of the difference between two
566 dependent correlations with one variable in common [Computer software]. Available from
567 <http://quantpsy.org>.
- 568 Lonfat, M., Rogers, R., Marchok, T., & Marks, F. D. (2007). A parametric model for predicting
569 hurricane rainfall. *Monthly Weather Review*, 135(9), 3086–3097.
570 <https://doi.org/10.1175/MWR3433.1>.
- 571 Maclay, K. S., DeMaria, M., Vonder Haar, T. H. (2008). Tropical cyclone inner-core kinetic
572 energy evolution. *Monthly Weather Review*, 136(12), 4882–4898,
573 <https://doi.org/10.1175/2008MWR2268.1>.
- 574 Mendelsohn, R., Emanuel, K., Chonabayashi, S., & Bakkensen, L. (2012). The impact of climate
575 change on global tropical cyclone damage. *Nature Climate Change*, 2, 205–209,
576 <https://doi.org/10.1038/nclimate1357>.
- 577 Misra, V., DiNapoli, S., & Powell, M. (2013). The track integrated kinetic energy of Atlantic
578 tropical cyclones. *Monthly Weather Review*, 141(7), 2383–2389, [https://doi.org/10.1175/MWR-](https://doi.org/10.1175/MWR-D-12-00349.1)
579 [D-12-00349.1](https://doi.org/10.1175/MWR-D-12-00349.1).
- 580 Powell, M. D., & Reinhold, T. A. (2007). Tropical cyclone destructive potential by integrated
581 kinetic energy. *Bulletin of the American Meteorological Society*, 88(4), 513–526,
582 <https://doi.org/10.1175/BAMS-88-4-513>.
- 583 Rappin, E. D., Nolan, D. S. & Majumdar, S. J. (2013). A highly configurable vortex initialization
584 method for tropical cyclones. *Monthly Weather Review*, 141(10), 3556–3575.
585 <https://doi.org/10.1175/MWR-D-12-00266.1>.
- 586 Schott, T., & Coauthors. (2012): The Saffir–Simpson hurricane wind scale. National Hurricane
587 Center, <http://www.nhc.noaa.gov/pdf/sshws.pdf>.
- 588 Simpson, R. H. (1974). The hurricane disaster potential scale. *Weatherwise*, 27(4), 169, 186,
589 <https://doi.org/10.1080/00431672.1974.9931702>.
- 590 Weinkle, J., Landsea, C., Collins, D., Masulin, R., Crompton, R. P., Klotzbach, P. J., & Pielke Jr.,
591 R. P. (2018). Normalized hurricane damage in the continental United States 1900–2017. *Nature*
592 *Sustainability*, 1(12), 808–813. <https://doi.org/10.1038/s41893-018-0165-2>

Characterizing Continental US Hurricane Risk: Which Intensity Metric is Best?

**Philip J. Klotzbach¹, Daniel R. Chavas², Michael M. Bell¹, Steven G. Bowen³,
Ethan J. Gibney⁴, and Carl J. Schreck III⁵**

¹Department of Atmospheric Science, Colorado State University, Fort Collins, CO, USA.

²Department of Earth, Atmospheric and Planetary Sciences, Purdue University, West Lafayette, IN, USA.

³Aon, Chicago, IL, USA.

⁴Cooperative Programs for the Advancement of Earth System Science, UCAR, San Diego, CA, USA.

⁵Cooperative Institute for Satellite Earth System Studies (CISESS), North Carolina State University, Asheville, NC, USA.

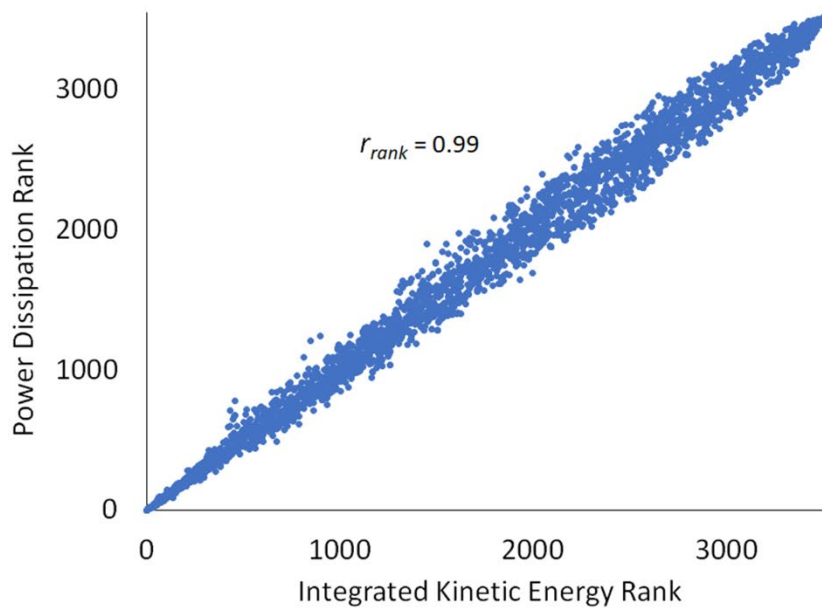
Contents of this file

Text S1
Figure S1
Table S1

Introduction

This supporting information includes brief additional text, one additional figure and one additional table. Text S1 discusses the physical reasoning behind the high correlation between IKE and PD. Figure S1 displays the relationship between IKE and PD from 1988–2020 for all Atlantic hurricanes and for southwest Atlantic hurricanes. Table S1 highlights the methodology used to calculate IKE in each quadrant.

(a)



(b)

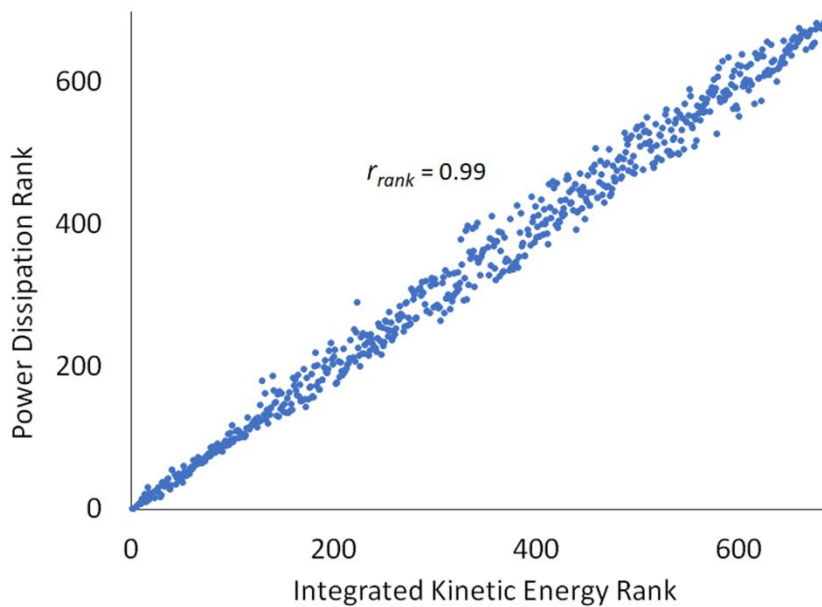


Figure S1. Relationship between PD and IKE. (a) Scatterplot of PD rank and IKE rank for all Atlantic hurricanes from 1988–2020. (b) As in panel a but for southwest Atlantic hurricanes from 2004–2020.

Table S1. Methodology for computing IKE in each quadrant at each 6-hourly timestep for each hurricane in the Extended Best Track database. The table format is identical to Table A1 from Misra et al. (2013). One adjustment is made for IKE_H to use three simple criteria; the criteria referencing “max quadrant” in their original methodology were unclear and unnecessary, and as a result the fourth criterion is no longer needed as it is subsumed in the previous three. All wind speeds are listed in units of ms^{-1} .

Quadrant IKE contribution	Criteria	Mean wind (ms^{-1})	Area (m^2)
IKE₁₈₋₂₆	$R_{26} > 0$	20	$0.25\pi(R_{18}^2 - R_{26}^2)$
	No R_{26} , $V_{max} > 26$, $R_{max} < R_{18}$	20	$0.25\pi(R_{18}^2 - (0.75R_{max})^2)$
	No R_{26} , $V_{max} < 26$, $R_{max} < R_{18}$	$0.25V_{max} + 0.75(18)$	$0.25\pi(R_{18}^2 - (0.75R_{max})^2)$
	No R_{26} , $R_{max} = R_{18}$	18	$0.25\pi(R_{18}^2 - (0.5R_{18})^2)$
IKE₂₆₋₃₃	$R_{33} > 0$	27.75	$0.25\pi(R_{26}^2 - R_{33}^2)$
	No R_{33} , $V_{max} > 33$, $R_{max} < R_{26}$	27.75	$0.25\pi(R_{26}^2 - (0.75R_{max})^2)$
	No R_{33} , $V_{max} < 33$, $R_{max} < R_{26}$	$0.25V_{max} + 0.75(26)$	$0.25\pi(R_{26}^2 - (0.75R_{max})^2)$
	No R_{33} , $R_{max} \geq R_{26}$	26	$0.25\pi(R_{26}^2 - (0.5R_{33})^2)$
IKE_H	$R_{max} < R_{33}$	$0.25V_{max} + 0.75(33)$	$0.25\pi(R_{33}^2 - (0.75R_{max})^2)$
	$R_{max} = R_{33}$	$0.25V_{max} + 0.75(33)$	$0.25\pi(R_{33}^2 - (0.75R_{33})^2)$
	$R_{max} > R_{33}$	$0.1V_{max} + 0.9(33)$	$0.25\pi(R_{33}^2 - (0.75R_{33})^2)$